

Article

Co-Pyrolysis of Woody Biomass and Oil Shale in a Batch Reactor in CO₂, CO₂-H₂O, and Ar Atmospheres

Alejandro Lyons Cerón * and Alar Konist 

Department of Energy Technology, Tallinn University of Technology, Ehitajate tee 5, 12616 Tallinn, Estonia

* Correspondence: allyon@taltech.ee

Abstract: The partial replacement of fossil fuels with biomass provides an alternative to producing cleaner and more sustainable energy and fuels. Conventional shale oil production infrastructure can potentially be used in co-pyrolysis with biomass to reduce the use of oil shale and decrease its environmental impact. The effect of adding 10 and 30 wt% woody biomasses (spruce, alder, pine, and birch) into oil shale was studied through intermediate co-pyrolysis. The experiments were carried out in a batch reactor at 520 °C, with a 20 min residence time, in CO₂, CO₂-H₂O 1:1, and Ar gas atmospheres. The solid products were collected and analyzed for elemental composition and surface area, while the composition of the gases was determined through gas chromatography. The difference in experimental and theoretical mass balances of fuel blends was lower than 2.5 wt% in all gas environments, indicating slight interactions between the fuels. CO₂ atmospheres contributed to increased decomposition, with up to 2.6 wt% lower solid products. Biomass increased the production of combustible gases, especially CO yields, from 0.42 to 1.30 vol%. The addition of biomass and the use of alternative atmospheres can improve pyrolysis through increased fuel decomposition and a lower share of residual mass from 74.4 wt% for oil shale to 58–70 wt% for oil shale and biomass blends.

Keywords: co-pyrolysis; batch reactor; oil shale; woody biomass



Citation: Lyons Cerón, A.; Konist, A. Co-Pyrolysis of Woody Biomass and Oil Shale in a Batch Reactor in CO₂, CO₂-H₂O, and Ar Atmospheres. *Energies* **2023**, *16*, 3145. <https://doi.org/10.3390/en16073145>

Academic Editors: Antonio Zuorro, Changkook Ryu, Athanasios I. Papadopoulos and Panos Seferlis

Received: 14 February 2023

Revised: 16 March 2023

Accepted: 29 March 2023

Published: 30 March 2023



Copyright: © 2023 by the authors. Licensee MDPI, Basel, Switzerland. This article is an open access article distributed under the terms and conditions of the Creative Commons Attribution (CC BY) license (<https://creativecommons.org/licenses/by/4.0/>).

1. Introduction

The use of conventional fossil fuels for energy solutions has produced a direct impact on the environment, increasing the emissions of greenhouse gases. This threatens to raise global temperatures above 1.5 °C by 2030 and 2050 [1]. Alternative and clean energy solutions can mitigate the environmental impact by reducing the emissions of pollutant gases and the depletion of non-renewable resources. The co-conversion of two types of resources such as biomass, a carbon-neutral renewable resource, and oil shale (OS), an alternative fuel, is proposed as a solution for the generation of more sustainable liquid, gaseous, and solid products through the partial replacement of OS with biomass in co-pyrolysis. Co-pyrolysis, a thermochemical conversion process, can produce valuable products (bio-oil, gas, porous char) for the energy sector and other industrial applications [2].

Biomass is a renewable non-fossil resource with a high carbon content, low ash content, high volatile matter, and a lower calorific value of 15–19 MJ/kg [3]. Its utilization can potentially provide 3000 TWh of energy and save 1.3 billion tons of CO₂ [4]. Biomass is composed of hemicellulose, cellulose, and lignin. Woody biomass (WB) is mostly composed of hemicellulose and cellulose (50–80 wt%) [5], which decompose at 220–315 °C and 350–400 °C [6], and the remaining component, lignin, decomposes at a temperature above 400 °C. The thermochemical conversion of WB through gasification or pyrolysis results in valuable products, such as bio-oil, gas, and porous char. From these processes, pyrolysis of biomass produces high yields of liquid (up to 75%), solid (10–25%), and gaseous products (20%) [7]. Intermediate pyrolysis is a relatively new conversion method, with a longer residence time, which yields around 40, 40, and 20 wt% of liquids, solids, and gas, respectively.

This process has been observed to have beneficial effects on reducing char cracking and a more stable bio-oil, while different research has proven beneficial effects of intermediate pyrolysis, including catalytic pyrolysis [8], and char with high thermal stability in N_2/CO_2 atmospheres [9]. However, there are some challenges in the individual conversion of WB. These are mostly due to its high moisture content and comparatively lower energy density than other fuels. WB energy density can be as low as one-tenth of a conventional fuel [10].

OS is an alternative fossil fuel obtained from geological formations in various locations around the world. It is characterized by its high share of organic matter (kerogen), which allows its use as an energy source through direct combustion, or as a source of valuable products, including shale oil, shale gas, and semi-coke. Depending on its type, OS has a lower calorific value in the range of 5–20 MJ/kg. The thermochemical conversion of OS results in up to 20% shale oil, 5–20% shale gas, and around 60% semi-coke [11]. During pyrolysis, OS kerogen is transformed into bitumen and further into liquid and gas products, such as volatile hydrocarbons, and solid products, such as semi-coke [12]. However, OS conversion also comes with environmental and technological challenges, such as reducing CO_2 emissions as well as NO_x and SO_x [13]. Various efforts have been made to transition from OS combustion to the production of shale oil [14], as its production is more profitable than the use of OS in power production.

Thermochemical conversion through co-pyrolysis involves two or more fuels, which undergo degradation in an oxygen-free atmosphere under specific thermal conditions, including temperature, residence time, and heating rate. This thermal degradation breaks the fuels' large molecules through different chemical reactions, producing liquid, solid, and gaseous products with combined properties from the pyrolyzed fuels [15]. Co-pyrolysis has been studied to determine the interactions between fuels, produce solid, liquid, and gaseous products with combined and/or improved properties, reduce the environmental effect of fossil fuels, and make use of waste residues [16]. The co-pyrolysis of fossil fuels, including OS, with shares of biomass, decreases the consumption of fossil fuels along with the emissions of pollutant gases from their individual conversion [17]. Due to its low ash content and high volatile matter, the addition of biomass to OS in co-pyrolysis can decrease the yields of solid products while increasing the yields of liquid and gaseous products [15]. Moreover, the high hydrogen content and H/C ratio of biomass can promote decomposition and thermal cracking in co-pyrolysis [18].

Possible interactions between biomass and other fuels have been observed to improve the pyrolytic behavior, shifting the pyrolysis temperature, reducing the activation energy of the process [19], and increasing the energy density [20]. Previous research on OS and biomass co-pyrolysis have found improvements in the decomposition and cracking of fuels, higher yields of pyrolysis products with enhanced properties, and lower CO_2 emissions [21]. The interactions and pyrolysis behavior of biomass and OS have been studied in TGA and different types of reactors in temperature ranges of 400–600 °C in inert atmospheres [22]. Some studies of OS co-pyrolysis have used OS and wheat straw [23], OS, and spirulina [24]. The effect of other atmospheres, such as CO_2 and steam, has been studied in gasification for biomass [25,26] but has not been studied in co-pyrolysis, even though such atmospheres have been demonstrated to have potential benefits in the decomposition of fuels, such as the pyrolysis of biomass in CO_2 [27]. Some of these benefits include enhanced pyrolysis [28], promotion of the liquid and gas product yields, prevention of secondary cracking (to produce more liquid products) [29], a decrease in the activation energy, a reduction of semi-coke and char yields, and bio-oil with improved properties [30].

Considering the possible advantages of the partial replacement of OS with biomass in co-pyrolysis and its potential to contribute to a path for cleaner energy solutions, the addition of shares of WB to OS in co-pyrolysis was studied using OS and forestry WB. For this purpose, experiments were carried out in a prototype batch reactor at isothermal conditions, at 520 °C for OS:WB blend ratios of 1:0, 9:1, 7:3, and 0:1. Different gas atmospheres, including Ar, CO_2 , and an $H_2O:CO_2$ blend were used to test their effect on the yield, elemental composition and surface area of solid products, and the concentration of

product gases, including CO, H₂, and CH₄. Solid products were collected to determine the residual mass, composition, and BET surface area, while the concentration of gas species was determined with gas chromatography with a thermal conductivity detector. Additionally, the individual pyrolysis of OS and WB was carried out at different residence times to study the decomposition of both fuels and determine the most suitable residence time for co-pyrolysis in the batch reactor to minimize the yield of solid products. The current study focused on solid and gaseous products, using a batch reactor designed for the production and collection of these products. The reactor's design does not allow an accurate collection of a representative sample of liquid products. Future work is required considering a larger-scale reactor to focus on liquid production and analysis.

2. Materials and Methods

2.1. Feedstock Characterization

The intermediate co-pyrolysis of biomass and OS was conducted using a blend of WB species; spruce, alder, pine, and birch from Estonian forests, and OS, a light-brown OS type also found in Estonia. The WB species were previously characterized [31] in terms of elemental and proximate composition and calorimetry according to ISO 16948, 16994, 18134-2, and 18122. OS was similarly characterized to obtain its elemental and proximate composition and calorific values according to ISO 29541:2015 and ISO 1928:2016 and EVS 669:1996 for the ash content. Details on the equipment used for elemental and proximate analysis and calorimetry are found in ref. [27]. The OS and the four types of WB species were individually sieved to a particle size between 0.5 and 1 mm, following the ISO 14780:20 (Solid biofuels—sample preparation) as a guideline. After sieving, the WB and OS samples were dried in a Nabertherm L9 furnace sourced from Nabertherm GmbH Lilienthal, Germany. The drying conditions were 105 °C for 3 h to remove moisture. Once the samples' moisture was removed, all WB samples were mixed in equal parts (25 wt% each) to obtain a blend of WB species. This WB blend was used to manually prepare blends of OS and WB with the following OS:WB ratios: 1:0, 9:1, 7:3, and 0:1 (0, 10, 30, and 100 wt% WB). The preparation of blends, as well as the storage in air plastic bags, was carried out following ISO 14780:20 guidelines. The analyses were conducted for WB, OS as raw feedstock and products of WB, OS, and blends after pyrolysis. After pyrolysis, the analysis was focused on the co-pyrolytic behavior of both feedstock and the composition of the solid products, including OS, WB, and OS-WB blends.

2.2. Experiment Set Up

The co-pyrolysis of blends of OS and WB was conducted in a prototype batch reactor, with a capacity of 1–5 g of fuel, at a reaction temperature of 520 °C in isothermal conditions. This temperature was chosen as it is the optimal temperature to obtain the highest yields of liquid products for OS and WB, or OS:WB blends [32]. The experiments were carried out in different gas atmospheres: Ar as an inert atmosphere, CO₂, and a blend of equal volumetric parts of CO₂ and H₂O (steam), with a total flow rate of 0.3 L/min. For each parameter, the experiment and 2 replicates were conducted to ensure reproducibility. The system used for the co-pyrolysis experiments (Figure 1) consisted of a batch reactor, a gas cleaning system, a gas analysis system, and a steam generator. The prototype batch reactor was composed of a balance chamber, where the sample holder containing the sample was inserted, and a reaction zone made of an internal heater with a precision of ±10 °C. A quartz cylindrical glass in the reaction zone contained the sample during the co-pyrolysis. A gas input supplied the gas atmosphere, controlled by Alicat Scientific Mass Flow controllers, with a precision of ±0.8%. A gas exhaust was used for the pyrolytic gas generated. The gas input and exhaust were externally heated to 150 °C to prevent condensation of volatiles in the system. Once the pyrolysis gas exited the reactor, it passed through a cooling and cleaning system operating at 4–6 °C to condensate volatiles. A Cole Parmer Steam Generator, sourced from Antylia Scientific in Vernon Hills, Illinois, United

States, was used to produce and deliver the steam for the CO₂:H₂O 1:1 atmosphere. The steam generator used N₂ as the carrier gas.

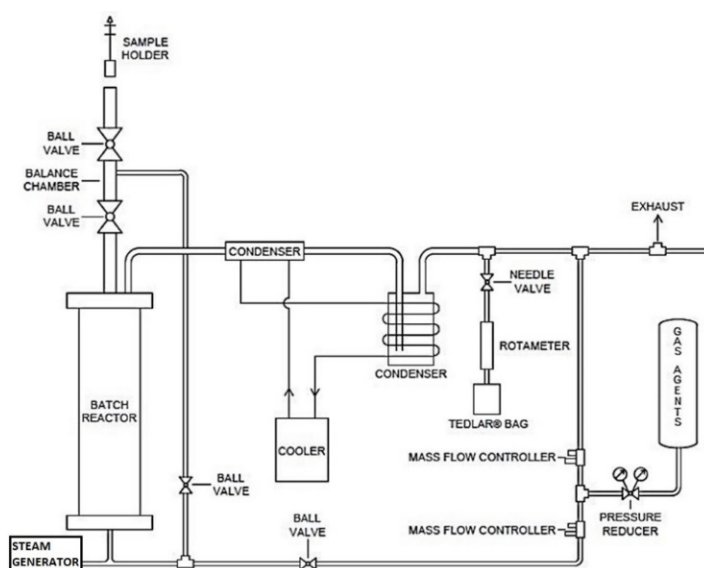


Figure 1. Pyrolysis system (modified from reference [33]).

Two types of experiments were conducted, both at 520 °C in isothermal conditions. The first type consisted of individual pyrolysis in an Ar atmosphere of 2.0 g ± 2.7% of OS and 1.5 g ± 1.1% of WB at different residence times in the reaction zone to study the evolution of the pyrolytic decomposition over time. For WB and OS, the residence times were 0.5, 1, 3, 5, 7, 10, and 20 min, and 2, 5, 10, 15, and 20 min, respectively. The second type of experiment was carried out in Ar, CO₂, and CO₂:H₂O 1:1 gas atmospheres to study co-pyrolysis of OS and WB, using 1.5 g ± 5.5% of OS:WB at 1:0, 9:1, 7:3, and 0:1 ratio. For the co-pyrolysis experiments, the residence time in the reaction zone was 20 min. Additionally, for both types of experiments, the samples were kept in the balance chamber before and after the reaction zone for 5 min to ensure an inert or clean atmosphere.

A comparison of the theoretical and experimental residual mass during the co-pyrolysis of OS:WB 9:1 and 7:3 was obtained from a linear correlation of OS and WB shares, based on the experimental residual mass of the individual pyrolysis of WB and OS (Equation (1)). m_{th} is the theoretical residual mass of OS:WB blends, m_{OS} and m_{WB} are the experimental residual mass of OS and WB, respectively, and x is the share of OS.

$$m_{th} = m_{OS}x + m_{WB}(1 - x) \quad (1)$$

2.3. Gas Products Analysis

The volumetric concentration of combustible gases H₂, CO, and CH₄ was measured using a gas chromatography with thermal conductivity detector (GC-TCD) and a Gazohrom 3101 gas analyzer. The analyzer was composed of two packed columns of 2.5 m in length and 3.6 mm in diameter and used air at 70 L/min as a carrier gas. The pyrolytic gas was collected in Tedlar bags after it exited the batch reactor and passed through the cleaning system. The GC-TCD was calibrated for the measured gas species, and the concentration in vol% was calculated using the chromatogram function of Clarity Software. The calibration of the GC-TCD is described in previous works with the same equipment [34].

2.4. Solid Product Analysis

The solid products obtained from the pyrolysis of OS and WB and OS:WB were evaluated for their elemental composition, using a Vario MACRO CHNS analyzer to determine the concentration of C, H, N, and S. The surface area of the solid products was

determined using a Quantachrome Autosorb iQ-C surface area and pore size analyzer, sourced from Anton Paar in Boynton Beach, Florida, United States, which determines the BET specific surface area, through physisorption. For these analyses, samples of 0.1–1.0 g of solid product were used. Firstly, the samples were put into degassing at 300 °C for 20 h to prepare, clean, and remove any volatiles from the samples. After degassing, the surface area was determined by recording 40 adsorption and 40 desorption points to obtain the isotherms, using N₂ as adsorbent gas.

3. Results and Discussion

3.1. Feedstock Properties

Table 1 displays the main properties of the WB and OS samples used, including elemental and proximate composition in terms of C, H, N, S, O, ash content, moisture content, fixed carbon, and volatile matter, as well as higher and lower calorific values (HHV and LHV, respectively). The values from the elemental analysis of WB and the organic part of OS were determined on a dry basis. All WB samples have a similar composition, making them suitable for studying their co-pyrolysis behavior as one blend of WB. As seen from Table 1, OS and WB differ in various aspects, particularly in their heating values, being over two-fold times higher for WB compared to OS, and the ash content, 0.3 wt% for WB and 52.5 wt% for OS. Therefore, it is expected to have a different pyrolytic behavior as well as residual mass for OS and WB and a combined pyrolytic behavior for OS:WB blends, according to the blend ratio.

Table 1. WB and OS feedstock properties.

		WB **				OS **
		Spruce	Alder	Pine	Birch	
Elemental composition [wt%]	C	50.3	49.9	50.1	49.3	27.2
	H	6.6	6.6	6.6	6.6	2.8
	N	0.1	0.2	0.19	0.08	<0.1
	S	n.d.	n.d.	n.d.	n.d.	2.0
	O *	42.7	43.0	43.1	44.0	21.0
Proximate analysis [wt%]	Ash content	0.3	0.3	0.3	0.3	52.5
	Moisture	6.9	7.6	8.5	7.7	0.9
	Fixed carbon	14.2	14.0	14.5	12.8	2.0
	Volatile matter	85.5	85.7	85.2	86.9	45.5
Heating value [MJ]/kg]	LHV	18.4	18.5	18.6	18.1	8.7
	HHV	19.8	19.9	20.0	19.9	9.7

* Calculated, ** dry-basis, n.d. not detected.

3.2. Pyrolysis at Different Residence Times

The pyrolytic behavior of WB and OS at 520 °C in the Ar atmosphere at different residence times is shown in Figure 2. The residual mass measurements obtained from pyrolysis experiments of WB and OS had a relative standard deviation of up to 2.88% and 2.29% for WB and OS, respectively, between each parameter and its replicates. Figure 2 indicates the difference in decomposition between WB and OS. WB samples were inserted in the reactor and removed after a residence time of 0.5, 1, 3, 5, 7, 10, and 20 min, as most of the reaction occurred during the initial 5 min. The residence time for OS samples was 2, 5, 10, 15, and 20 min, considering the slower decomposition of OS. The results shown in Figure 2 were used to set the most suitable residence time for the co-pyrolysis of OS and WB so that the blend of fuels achieved a complete decomposition for the pyrolysis temperature considered (520 °C).

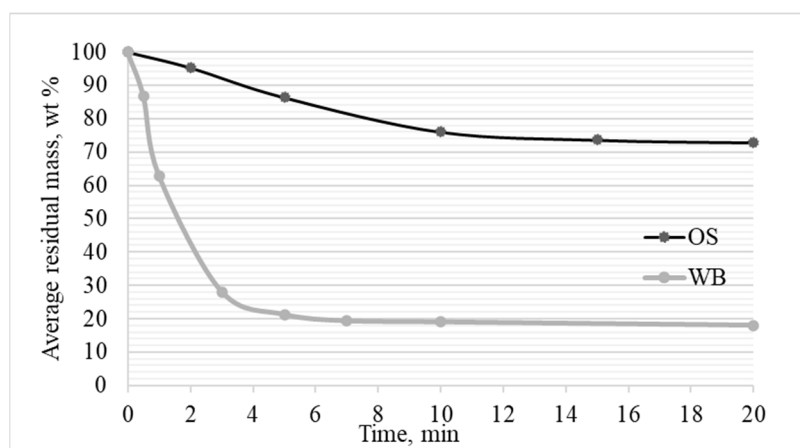


Figure 2. Residual mass from individual pyrolysis of OS and WB.

The pyrolysis of WB at different resident times indicated that over 95% of the decomposition occurred during the first 5 min of the reaction process, where WB lost over 78 wt% of its mass, reaching a residual mass of 21.2 wt%. After 5 min, the mass loss only increased by 3.2 wt% in 15 min, reaching a residual mass of 18.0 wt% at a residence time of 20 min. This residual mass after 20 min consisted of char, ashes, and some residual mass from incomplete pyrolysis (4 wt%). This behavior showed that during the first 5 min of the reaction, the WB samples reached temperatures close to 400 °C, where its main components decomposed, starting with cellulose and hemicellulose from 0–5 min and lastly lignin, which likely occurred within 3–5 min of the reaction. The composition of WB in terms of cellulose, hemicellulose, and lignin explains the reason most of WB mass was decomposed within the first 7 min of the pyrolysis, as the sample reached the temperature of the reactor (520 °C). At this temperature, the WB samples underwent most of the pyrolysis due to the decomposition temperatures of these three components. Mass losses occurring after 5–7 min (below 2.0 wt% mass loss) can be considered decomposition from incomplete pyrolysis of hemicellulose and cellulose of the WB samples; with the decomposition of lignin, the complete decomposition of WB occurs at 800–900 °C [5]. Similar observations have been noted by refs. [35,36]. Based on these results, it is observed that WB in the batch reactor requires a residence time of no less than 7 min. Residence times above 10 min will not increase the mass loss by more than 1–2 wt%. Additional evidence of this behavior is shown in Appendix A.1, which visually displays the solid residues of WB after different residence times. The residues indicate that after 3–5 min, most of the residue is char, while before 3 min, there is still a share of unreacted WB.

The case for OS differs from WB pyrolytic behavior. As Figure 2 shows, OS has a linear decomposition during 0–10 min of the reaction, where it is subject to a mass loss of 23.9 wt%, reaching 76.1 wt% residual mass at a 10 min residence time. This mass loss represents over 86% of the total maximum mass loss during pyrolysis at 20 min residence time. After 10 min, OS lost 3.2 wt% of its mass in the remaining 10 min. The residual mass from OS pyrolysis is composed of semicoke, which is OS that has lost a portion of hydrocarbons; moreover, the complete decomposition of OS occurs within the range of 540–900 °C [37]; therefore, the residual mass of 72.9 wt% is higher than the ash + fixed carbon of OS from the elemental analysis. Unlike WB, OS decomposition was slower, indicating that the fuel required more time to reach the temperature range where most of the decomposition occurs (350–510 °C). During the first 10 min of the reaction, OS Kerogen was transformed into its products: shale oil, gas, and semi-coke. Further decomposition can be attributed to the completion of pyrolysis, and the decomposition of incomplete pyrolysis, after which the fuel reaches the operating temperature of the reactor (520 °C). This behavior agrees with observations by refs. [11,38,39], who studied the kinetic and thermogravimetric behavior of OS. Therefore, for the pyrolysis of OS in the batch reactor, it is required that the residence time is greater than 15 min to achieve maximum decomposition for the selected

operating temperature. Residence times above 15 min will not increase the mass loss by more than 1–2 wt%. Appendix A.2 contains visual evidence of the OS decomposition at different residence times, indicating the required residence time above 15 min to transform OS into semi-coke. Based on the obtained results, a residence time of 20 min was chosen for the co-pyrolysis of OS and WB to ensure maximum decomposition of both fuels.

3.3. OS-WB Co-Pyrolysis

Figure 3 displays the residual mass from individual pyrolysis of OS and WB and co-pyrolysis of OS:WB 9:1 and 7:3 in Ar, CO₂, and H₂O:CO₂ 1:1 atmospheres. The residual mass measurements obtained from co-pyrolysis experiments of WB and OS had a relative standard deviation from 0.35% up to 3.99% between each parameter and its replicates. The addition of 10 and 30 wt% WB to OS (blends 9:1 and 7:3) decreased the residual mass as the share of WB rose. This resulted in a residual mass of 57.4–60.0 wt% and 68.2–71.6 wt% for OS:WB blends of 7:3 and 9:1, respectively, in all gas atmospheres. The results were compared to the theoretical curves of OS:WB co-pyrolysis formulated using Equation (1), as shown in detail in Figure 3 for all the tested gas atmospheres. Overall, the comparison of residual masses evidences the additive decomposition behavior of OS:WB in co-pyrolysis, as the experimental results share a linear decrease in residual mass as the ratio of WB increases.

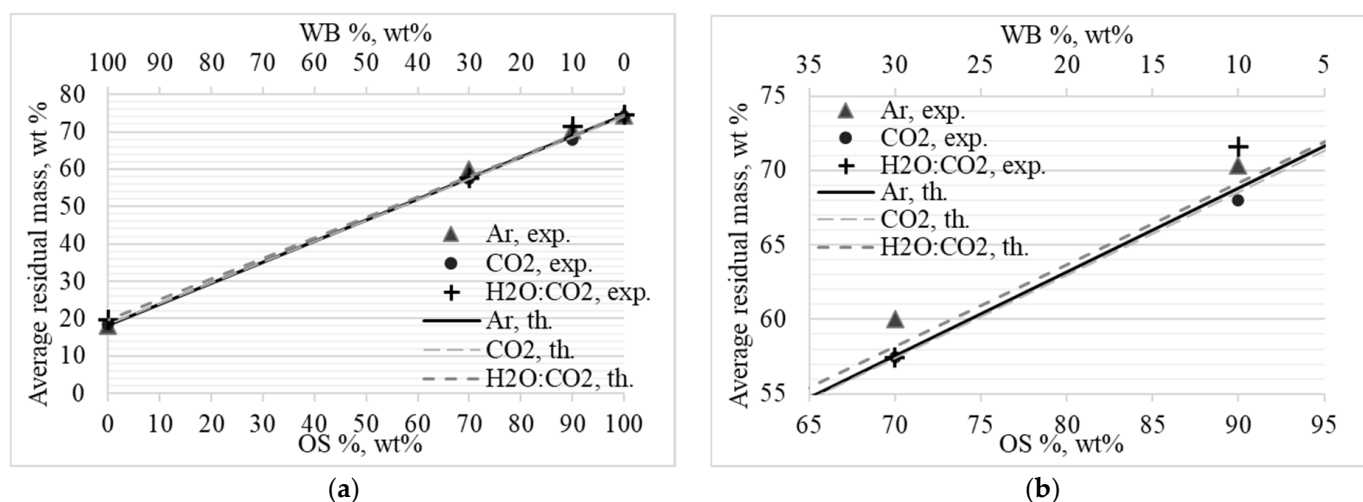


Figure 3. (a) Theoretical (th.) co-pyrolysis curves and experimental results (exp.). (b) Detail of theoretical (th.) and experimental (exp.) residual mass for co-pyrolysis blends.

The experimental residual mass obtained had a behavior comparable to the theoretical curves, with a difference lower than 2.5 wt%, indicating the absence of strong promoting or inhibiting effects between the two fuels. This absence of strong interactions was also observed by refs. [40–42]. Johannes et al. [40] co-pyrolyzed OS and pine sawdust, resulting in a synergistic effect in the yield of oil (21% more); however, this was observed only during incomplete pyrolysis at temperatures below 360 °C, where the pyrolysis process is still ongoing. At higher temperatures, there was no synergy in co-pyrolysis. Yanik et al. [41] found that the co-pyrolysis of OS with berries had an additive result in the total extract yield. At 400 °C, the yield of organic residue was 41.47 and 32.47 wt%, respectively, for OS and berries, while the co-pyrolysis yield was 36.46 wt%, which is almost identical to the theoretical yield of 36.97 wt%. Kılıç et al. [42] conducted co-pyrolysis of OS with *Euphorbia rigida*, resulting in no significant synergistic effect. The solid yields at 550 °C were 26.87 and 16.66% for OS and *E.rigida*, respectively. The co-pyrolysis yield was from 20–22%, which is not different from the theoretical yield of 21.76%. Additionally, the liquid product was an additive result of both feedstocks.

Despite the absence of strong interactions between OS and WB in the current experiments, the addition of WB to OS pyrolysis has the potential to improve the decomposition of OS as well as improve its products. In co-pyrolysis with WB, OS decomposition is shifted to a lower temperature region, resulting in earlier decomposition due to the lower temperatures required to pyrolyze WB components, which products can interact with OS. Some of the WB components that interact with OS include hydrogen-free radicals (considering the higher H content of biomass, shown in Table 1). These radicals can promote kerogen and bitumen cracking and WB inorganic elements, which can produce a catalytic effect on OS and enhance its decomposition. From the current experiments, a direct advantage is observed with the addition of 30 wt% WB to OS in co-pyrolysis, as the residual mass decreases the most with this WB share. Higher shares of WB decrease the share of semi-coke produced from OS retorting and the environmental effects of OS pyrolysis, such as emissions of NO_x , SO_x , and CO_2 , as also observed by ref. [42]. Other studies with biomass in co-pyrolysis with coal have observed strong interactions, especially in the devolatilization rate, the generation of CO_2 , and improved pyrolysis through volatile–char interactions [43]. Moreover, benefits are also observed for WB in co-pyrolysis, as blends of OS and WB result in fuel mixtures with a higher energy density and lower moisture content than the individual pyrolysis of WB.

Figure 3 also displays the differences in residual mass as the gas atmosphere varies in Ar inert atmosphere, CO_2 , and the $\text{H}_2\text{O}:\text{CO}_2$ 1:1 blend. It was observed that the co-pyrolysis of OS:WB in all gas environments followed a linear behavior, decreasing the residual mass as the WB share increased, with a linear coefficient of determination R^2 in the range of 0.997–0.999 for all gas atmospheres. On average, the residual masses were 18.8, 58.3, 70.0, and 74.4 wt% for OS:WB blends of 0:1, 7:3, 9:1, and 1:0, respectively, with an RSD between gas atmospheres in the range of 0.3 to 4.6%. This indicates slight differences in the decomposition of OS:WB blends as the gas atmosphere varied. Nevertheless, the co-pyrolysis in non-inert atmospheres resulted in a lower residual mass for OS:WB blends 7:3, 9:1, and 1:0 in CO_2 and for OS:WB blends 7:3 in $\text{H}_2\text{O}:\text{CO}_2$. Non-inert atmospheres, such as CO_2 and $\text{H}_2\text{O}:\text{CO}_2$ blends, have led to a pyrolytic decomposition comparable to or, in some cases, improved compared to Ar as an inert atmosphere. This is likely due to the role of CO_2 and H_2O in pyrolysis. CO_2 can enhance thermal efficiency, cracking, and improve decomposition, while H_2O can act as a reactive agent and promote secondary cracking and provide free hydrogen radicals. For the experimental conditions used, CO_2 and H_2O did not promote gasification reactions, as the reaction temperature was below 700 °C. Above 700 °C, CO_2 and H_2O play a major role in the process, specifically in the Boudouard, water–gas, and water–gas shift reactions [34]. The similarities and improvements in the co-pyrolytic decomposition of OS:WB blends allow the implementation of CO_2 and H_2O atmospheres as a feasible alternative to inert atmospheres in the co-pyrolysis of OS:WB blends. Using such gas atmospheres, especially CO_2 , can potentially make use of CO_2 emissions captured through carbon capture and storage (CCS) technologies [44], addressing the environmental impact of CO_2 emissions.

3.4. Gas Composition

The concentration of H_2 , CO , and CH_4 obtained from the co-pyrolysis gas is shown in Table 2. Every Tedlar gas sample for a single experiment was measured three times with an average error from 0.9–12.9%, 0.7–15.4%, 1.8–12.8%, and 1.5–12.1% for WB, OS, OS:WB 7:3, and OS:WB 9:1, respectively. Every experiment was conducted three times, with an average standard deviation between parallel experiments of 1.6–25.0%, 2.7–24.1%, and 2.7–27% for H_2 , CO , and CH_4 , respectively. Other uncertainties in GC-TCD can be related to the injection of the gas, measurement repeatability, column temperature [45], and the collection of the gas sample from the reactor, among others. Higher deviation in the gas analysis is related to the lower concentration of gases obtained rather than the reproducibility of the experiment. Evidence of this is the low deviation in the yield of solid products (lower than 5%). The presence of the three combustible gases was significantly

low in comparison to other thermochemical conversion processes, such as gasification. This is due to the lower decomposition temperature selected, aimed to decrease secondary cracking. Higher pyrolysis temperatures could have increased the H₂, CO, and CH₄ due to reduction reactions occurring above 600 °C, converting more fuel into gas products and transforming CO₂ into CO [46]. In general, the concentration of H₂, CO, and CH₄ was higher in the individual pyrolysis of WB, especially that of CO and CH₄, due to the elemental composition of the fuel. There was no clear correlation between the concentration of gas species and the ratio of OS:WB blends. Nonetheless, the concentration of gas species was in a low range to provide any clear relation. The effect of the gas atmosphere on the produced gases had no clear trend or difference between CO₂, H₂O:CO₂ 1:1, and Ar atmospheres. The gas concentration of H₂, CO, and CH₄ is not significantly different between atmospheres due to the low pyrolysis temperature, where the atmospheres do not have a strong interaction with the feedstock [34]. The largest share of gas species in the pyrolysis gas was the species used as the gas atmosphere (Ar, CO₂, or H₂O:CO₂). It should be noted that during pyrolysis, other gas species are produced, including CO₂, NO_x, SO_x, and other hydrocarbons. The equipment used had calibration and capabilities to measure only H₂, CO, and CH₄.

Table 2. Concentration of H₂, CO, and CH₄ in the co-pyrolysis gas.

OS:WB Ratio	Gas Atmosphere, 0.3 L/min	Gas Species Concentration, vol%		
		H ₂	CO	CH ₄
0:1	CO ₂	0.08	1.19	0.15
	H ₂ O:CO ₂ 1:1	0.06	1.01	0.14
	Ar	0.08	1.30	0.14
7:3	CO ₂	0.05	0.56	0.06
	H ₂ O:CO ₂ 1:1	0.07	0.87	0.04
	Ar	0.05	0.82	0.07
9:1	CO ₂	0.05	0.31	0.08
	H ₂ O:CO ₂ 1:1	0.05	0.37	0.04
	Ar	0.06	0.65	0.06
1:0	CO ₂	0.06	0.42	0.06
	H ₂ O:CO ₂ 1:1	0.1	0.75	0.06
	Ar	0.04	0.42	0.05

3.5. Solid Products

Table 3 displays the characteristics of the solid products obtained from individual pyrolysis and co-pyrolysis of OS and WB and OS:WB blends. It is observed how the composition of the solid products is directly related to the elemental composition of WB and OS, with WB char having a higher content of C, H, and N, which gradually decreases as the share of WB decreases. In parallel, the share of S is only observable in blends with OS due to the high sulfur content of OS. It should also be considered that from individual pyrolysis, the share of residual mass is close to 19 and 74 wt% for WB and OS, respectively. This means that for the OS:WB blends studied, most of the residual mass is composed of OS semi-coke, which explains why the elemental composition of these blends is similar to the composition of OS semi-coke. Therefore, OS has a more significant contribution in the composition of the solid products in OS:WB co-pyrolysis, while WB has a larger contribution in the production of gaseous and liquid products. The blend of OS:WB should then be selected based on what type of product needs to be obtained in the co-pyrolysis process. Similarly, the BET-specific surface areas obtained through physisorption are shown in Table 3. The BET surface area results show how considerably higher values for WB solid products (127–173 m²/g) compared to OS and OS:WB blends (4–46 m²/g). It is known that biochar, obtained from biomass, usually has a surface area ranging from 8–132 m²/g [47], while OS semi-coke has a surface area of around 4–50 m²/g [48]. As with the elemental

composition of solid products, the surface area of OS:WB blends is comparable to the one obtained from individual pyrolysis of OS due to the higher contribution of OS semi-coke in the blend. The effect of the gas atmosphere on the elemental composition and surface area of the solid residues did not show a clear difference or trend in the results obtained in CO₂, H₂O:CO₂ 1:1, and Ar atmospheres. As with the solid yields in co-pyrolysis, the similarities of the results in all atmospheres are related to the lower pyrolysis temperature used, at which the CO₂ and H₂O gases have low interaction with the feedstock, as explained by the main reduction reactions of CO₂ and H₂O [34]. Future suggestions for increasing the specific surface area of the blends include pyrolyzing blends with higher shares of WB and optimizing the pyrolysis parameters, including temperature, heating rate, pressure, residence time, and post-treatments [47].

Table 3. Elemental composition of OS, WB, and OS:WB solid products, BET surface area of solid products.

OS:WB Ratio	Gas Atmosphere, 0.3 L/min	C, wt%	H, wt%	N, wt%	S, wt%	BET, m ² /g
0:1	CO ₂	78.92	3.26	0.40	n.d. *	127.9
	H ₂ O:CO ₂ 1:1	78.86	3.47	0.38	n.d.	173.8
	Ar	77.29	3.39	0.43	n.d.	175.9
7:3	CO ₂	15.03	0.27	0.05	0.69	17.8
	H ₂ O:CO ₂ 1:1	15.87	0.40	0.04	0.69	19.5
	Ar	14.39	0.27	0.05	1.09	6.1
9:1	CO ₂	12.00	0.15	0.02	0.72	19.1
	H ₂ O:CO ₂ 1:1	12.64	0.20	0.02	0.95	29.3
	Ar	11.77	0.19	0.02	1.87	45.7
1:0	CO ₂	11.39	0.22	0.02	1.12	11.4
	H ₂ O:CO ₂ 1:1	11.25	0.20	0.01	0.94	28.8
	Ar	11.55	0.20	0.01	0.90	4.3

* n.d. not detected.

4. Conclusions

This work studied the effect of adding shares of woody biomass to oil shale pyrolysis using a batch reactor in isothermal conditions and with various gas atmospheres. The residual masses yields, composition, surface area, and produced gas yields were analyzed to determine the interactions and effects of both fuels in co-pyrolysis.

An optimal residence time of 20 min for co-pyrolysis was defined through the results of individual pyrolysis of each fuel. Due to its higher pyrolysis temperature, OS decomposition occurred slower than WB (90% decomposition in 15 min compared to 95% in 5 min for the reactor used). As WB reaches the isothermal temperature faster, it can contribute to the pyrolysis of OS, accelerating its decomposition.

The residual mass of OS:WB co-pyrolysis indicates an additive behavior, as it linearly decreases as the share of WB raises, with less than a 2.5 wt% difference between theoretical and experimental yields of solid products. Despite the evidence of strong interactions, adding WB to OS results in lower production of solids compared to individual pyrolysis of OS, reducing its environmental impact, while similarly, adding OS to WB increases the energy density of the blend.

All gas atmospheres had a comparable linear behavior, decreasing the residual mass as the WB ratio increased. Despite improvements in non-inert atmospheres (<2.6 wt% difference) compared to Ar co-pyrolysis, CO₂ and H₂O:CO₂ proved to yield solid products as low or lower than pyrolysis in Ar inert atmosphere, indicating its potential to use CO₂ from CCS in co-pyrolysis.

The BET-specific surface area was observed to be higher for WB solid products and comparable to OS semi-coke for OS:WB blends. To increase the surface area in blends, it would be necessary to use higher shares of WB, optimize the pyrolysis parameters, or use post-treatment methods.

Future research can address the effect of OS:WB co-pyrolysis in the yield and composition of liquid products, considering their potential use as valuable biofuels. Additionally, OS:WB blend ratios with higher shares of WB and the characterization of the liquid products could contribute to a better understanding of the co-pyrolytic behavior. Future experimental arrangements in larger scale reactors and/or prototype reactors can contribute to the state of the art of co-pyrolysis, leading to valuable results for industrial applications.

Author Contributions: Conceptualization, A.L.C. and A.K.; methodology, A.L.C. and A.K.; software, A.L.C.; validation, A.L.C. and A.K.; formal analysis A.L.C. and A.K.; writing—original draft preparation, A.L.C.; writing—review and editing, A.L.C. and A.K.; visualization, A.L.C.; supervision, A.K. All authors have read and agreed to the published version of the manuscript.

Funding: This work was supported by the European Regional Development Fund and the Estonian Research Council Grant (PSG266).

Data Availability Statement: Data are not publicly available; the data may be made available upon request from the corresponding author.

Conflicts of Interest: The authors declare no conflict of interest.

Nomenclature

BET	Brunauer, Emmett, and Teller surface area
CCS	Carbon capture and storage technologies
GC-TCD	Gas chromatography with thermal conductivity detector
HHV	Gross or higher heating value
LHV	Net or lower heating value
OS	Oil shale
TGA	Thermogravimetric analysis
WB	Woody biomass

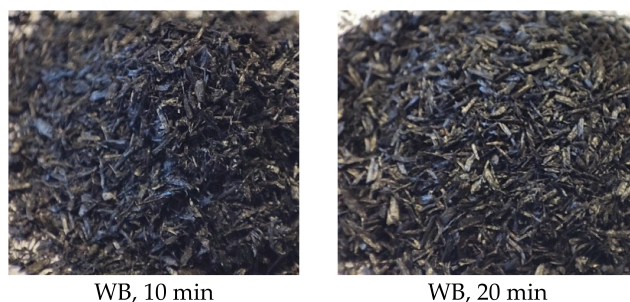
Appendix A

Appendix A.1

Raw WB and WB residues after decomposition in the batch reactor, with different residence times.

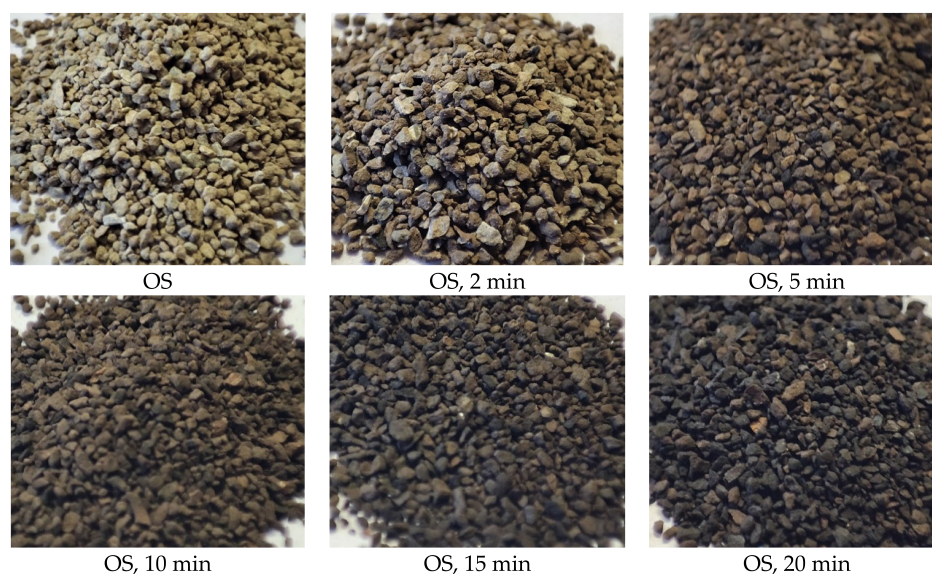


Figure A1. Cont.



Appendix A.2

Raw OS and OS residues after decomposition in the batch reactor, with different residence times.



References

1. Rogelj, J.; Den Elzen, M.; Höhne, N.; Fransen, T.; Fekete, H.; Winkler, H.; Schaeffer, R.; Sha, F.; Riahi, K.; Meinshausen, M. Paris Agreement climate proposals need a boost to keep warming well below 2 °C. *Nature* **2016**, *534*, 631–639. [[CrossRef](#)] [[PubMed](#)]
2. Mariyam, S.; Shahbaz, M.; Al-Ansari, T.; Mackey, H.R.; McKay, G. A critical review on co-gasification and co-pyrolysis for gas production. *Renew. Sustain. Energy Rev.* **2022**, *161*, 112349. [[CrossRef](#)]
3. Zhang, L.; Xu, C.; Champagne, P. Overview of recent advances in thermo-chemical conversion of biomass. *Energy Convers. Manag.* **2010**, *51*, 969–982. [[CrossRef](#)]
4. Antar, M.; Lyu, D.; Nazari, M.; Shah, A.; Zhou, X.; Smith, D.L. Biomass for a sustainable bioeconomy: An overview of world biomass production and utilization. *Renew. Sustain. Energy Rev.* **2021**, *139*, 110691. [[CrossRef](#)]
5. Wang, S.; Luo, Z. *Pyrolysis of Biomass*; GREEN—Alternative Energy Resources; Walter de Gruyter GmbH: Berlin, Germany, 2017; p. 268.
6. Akhtar, A.; Krepl, V.; Ivanova, T. A combined overview of combustion, pyrolysis, and gasification of biomass. *Energy Fuels* **2018**, *32*, 7294–7318. [[CrossRef](#)]
7. Uddin, M.N.; Techato, K.; Taweekun, J.; Rahman, M.M.; Rasul, M.G.; Mahlia, T.M.I.; Ashrafur, S.M. An overview of recent developments in biomass pyrolysis technologies. *Energies* **2018**, *11*, 3115. [[CrossRef](#)]
8. Jerzak, W.; Gao, N.; Kalembe-Rec, I.; Magdziarz, A. Catalytic intermediate pyrolysis of post-extraction rapeseed meal by reusing ZSM-5 and Zeolite Y catalysts. *Catal. Today* **2022**, *404*, 63–77. [[CrossRef](#)]
9. Ibrahim, M.D.; Abakr, Y.A.; Gan, S.; Lee, L.Y.; Thangalazhy-Gopakumar, S. Intermediate Pyrolysis of Bambara Groundnut Shell (BGS) in Various Inert Gases (N₂, CO₂, and N₂/CO₂). *Energies* **2022**, *15*, 8421. [[CrossRef](#)]
10. Wang, Q.; Li, X.; Wang, K.; Zhu, Y. Commercialization and challenges for the next generation of biofuels: Biomass fast pyrolysis. In Proceedings of the 2010 APPEEC Conference, Chengdu, China, 28–31 March 2010; IEEE: Piscataway, NJ, USA, 2010; pp. 1–4.
11. Bai, F.; Sun, Y.; Liu, Y.; Li, Q.; Guo, M. Thermal and kinetic characteristics of pyrolysis and combustion of three oil shales. *Energy Convers. Manag.* **2015**, *97*, 374–381. [[CrossRef](#)]

12. Raja, M.A.; Zhao, Y.; Zhang, X.; Li, C.; Zhang, S. Practices for modeling oil shale pyrolysis and kinetics. *Rev. Chem. Eng.* **2017**, *34*, 21–42. [[CrossRef](#)]
13. Ristic, N.D.; Djokic, M.R.; Konist, A.; Van Geem, K.M.; Marin, G.B. Quantitative compositional analysis of Estonian shale oil using comprehensive two dimensional gas chromatography. *Fuel Process. Technol.* **2017**, *167*, 241–249. [[CrossRef](#)]
14. Maaten, B.; Järvi, O.; Pihl, O.; Konist, A.; Siirde, A. Oil shale pyrolysis products and the fate of sulfur. *Oil Shale* **2020**, *37*, 51–69. [[CrossRef](#)]
15. Jin, Q.; Wang, X.; Li, S.; Mikulčić, H.; Bešenić, T.; Deng, S.; Vujanović, M.; Tan, H.; Kumfer, B.M. Synergistic effects during co-pyrolysis of biomass and plastic: Gas, tar, soot, char products and thermogravimetric study. *J. Energy Inst.* **2019**, *92*, 108–117. [[CrossRef](#)]
16. Ganev, E.; Ivanov, B.; Vaklieva-Bancheva, N.; Kirilova, E.; Dzhelil, Y. A multi-objective approach toward optimal design of sustainable integrated biodiesel/diesel supply chain based on first-and second-generation feedstock with solid waste use. *Energies* **2021**, *14*, 2261. [[CrossRef](#)]
17. Li, S.; Chen, X.; Liu, A.; Wang, L.; Yu, G. Co-pyrolysis characteristic of biomass and bituminous coal. *Bioresour. Technol.* **2015**, *179*, 414–420. [[CrossRef](#)] [[PubMed](#)]
18. Krerkkaiwan, S.; Fushimi, C.; Tsutsumi, A.; Kuchonthara, P. Synergetic effect during co-pyrolysis/gasification of biomass and sub-bituminous coal. *Fuel Process. Technol.* **2013**, *115*, 11–18. [[CrossRef](#)]
19. Özsın, G.; Püttin, A.E. TGA/MS/FT-IR study for kinetic evaluation and evolved gas analysis of a biomass/PVC co-pyrolysis process. *Energy Convers. Manag.* **2019**, *182*, 143–153. [[CrossRef](#)]
20. Kong, L.; Li, G.; Jin, L.; Hu, H. Pyrolysis behaviors of two coal-related model compounds on a fixed-bed reactor. *Fuel Process. Technol.* **2015**, *129*, 113–119. [[CrossRef](#)]
21. Jiang, H.; Deng, S.; Chen, J.; Zhang, L.; Zhang, M.; Li, J.; Li, S.; Li, J. Preliminary study on co-pyrolysis of spent mushroom substrate as biomass and Huadian oil shale. *Energy Fuels* **2016**, *30*, 6342–6349. [[CrossRef](#)]
22. Cerón, A.L.; Konist, A.; Lees, H.; Järvi, O. Current status of co-pyrolysis of oil shale and biomass. *Oil Shale* **2021**, *38*, 228–263. [[CrossRef](#)]
23. Chen, B.; Han, X.; Mu, M.; Jiang, X. Studies of the co-pyrolysis of oil shale and wheat straw. *Energy Fuels* **2017**, *31*, 6941–6950. [[CrossRef](#)]
24. Dai, M.; Yu, Z.; Fang, S.; Ma, X. Behaviors, product characteristics and kinetics of catalytic co-pyrolysis spirulina and oil shale. *Energy Convers. Manag.* **2019**, *192*, 1–10. [[CrossRef](#)]
25. Nowicki, L.; Siuta, D.; Markowski, M. Carbon Dioxide Gasification Kinetics of Char from Rapeseed Oil Press Cake. *Energies* **2020**, *13*, 2318. [[CrossRef](#)]
26. Nowicki, L.; Siuta, D.; Markowski, M. Pyrolysis of rapeseed oil press cake and steam gasification of solid residues. *Energies* **2020**, *13*, 4472. [[CrossRef](#)]
27. Ye, J.; Xiao, J.; Huo, X.; Gao, Y.; Hao, J.; Song, M. Effect of CO₂ atmosphere on biomass pyrolysis and in-line catalytic reforming. *Int. J. Energy Res.* **2020**, *44*, 8936–8950. [[CrossRef](#)]
28. Giudicianni, P.; Cardone, G.; Ragucci, R. Cellulose, hemicellulose and lignin slow steam pyrolysis: Thermal decomposition of biomass components mixtures. *J. Anal. Appl. Pyrolysis* **2013**, *100*, 213–222. [[CrossRef](#)]
29. Kantarelis, E.; Yang, W.; Blasiak, W. Production of liquid feedstock from biomass via steam pyrolysis in a fluidized bed reactor. *Energy Fuels* **2013**, *27*, 4748–4759. [[CrossRef](#)]
30. Lee, J.; Yang, X.; Cho, S.H.; Kim, J.K.; Lee, S.S.; Tsang, D.C.W.; Ok, Y.S.; Kwon, E.E. Pyrolysis process of agricultural waste using CO₂ for waste management, energy recovery, and biochar fabrication. *Appl. Energy* **2017**, *185*, 214–222. [[CrossRef](#)]
31. Sulg, M.; Konist, A.; Järvi, O. Characterization of different wood species as potential feedstocks for gasification. *Agron. Res.* **2021**, *19*, 276–299.
32. Chen, B.; Han, X.; Tong, J.; Mu, M.; Jiang, X.; Wang, S.; Shen, J.; Ye, X. Studies of fast co-pyrolysis of oil shale and wood in a bubbling fluidized bed. *Energy Convers. Manag.* **2020**, *205*, 112356. [[CrossRef](#)]
33. Cascante Cirici, P. Biomass and Oil Shale Co-Pyrolysis. Master's Thesis, Tallinn University of Technology, Tallinn, Estonia, 2019.
34. Cerón, A.L.; Konist, A.; Lees, H.; Järvi, O. Effect of woody biomass gasification process conditions on the composition of the producer gas. *Sustainability* **2021**, *13*, 11763. [[CrossRef](#)]
35. Garcia-Perez, M.; Wang, X.S.; Shen, J.; Rhodes, M.J.; Tian, F.; Lee, W.J.; Wu, H.; Li, C.Z. Fast pyrolysis of oil mallee woody biomass: Effect of temperature on the yield and quality of pyrolysis products. *Ind. Eng. Chem. Res.* **2008**, *47*, 1846–1854. [[CrossRef](#)]
36. Grieco, E.; Baldi, G. Analysis and modelling of wood pyrolysis. *Chem. Eng. Sci.* **2011**, *66*, 650–660. [[CrossRef](#)]
37. Syed, S.; Qudaih, R.; Talab, I.; Janajreh, I. Kinetics of pyrolysis and combustion of oil shale sample from thermogravimetric data. *Fuel* **2011**, *90*, 1631–1637. [[CrossRef](#)]
38. Tiwari, P.; Deo, M. Compositional and kinetic analysis of oil shale pyrolysis using TGA-MS. *Fuel* **2012**, *94*, 333–341. [[CrossRef](#)]
39. Tiwari, P.; Deo, M. Detailed kinetic analysis of oil shale pyrolysis TGA data. *AIChE J.* **2012**, *58*, 505–515. [[CrossRef](#)]
40. Johannes, I.; Tiikma, L.; Luik, H. Synergy in co-pyrolysis of oil shale and pine sawdust in autoclaves. *J. Anal. Appl. Pyrolysis* **2013**, *104*, 341–352. [[CrossRef](#)]
41. Yanik, J.; Secim, P.; Karakaya, S.; Tiikma, L.; Luik, H.; Krasulina, J.; Raik, P.; Palu, V. Low-temperature pyrolysis and co-pyrolysis of Göynük oil shale and terebinth berries (Turkey) in an autoclave. *Oil Shale* **2011**, *28*, 469–486. [[CrossRef](#)]

42. Kiliç, M.; Pütün, A.E.; Uzun, B.B.; Pütün, E. Converting of oil shale and biomass into liquid hydrocarbons via pyrolysis. *Energy Convers. Manag.* **2014**, *78*, 461–467. [[CrossRef](#)]
43. Tian, B.; Wang, J.; Qiao, Y.; Huang, H.; Xu, L.; Tian, Y. Understanding the pyrolysis synergy of biomass and coal blends based on volatile release, kinetics and char structure. *Biomass Bioenergy* **2023**, *168*, 106687. [[CrossRef](#)]
44. Cheng, C.-Y.; Kuo, C.-C.; Yang, M.-W.; Zhuang, Z.-Y.; Lin, P.-W.; Chen, Y.-F.; Yang, H.-S.; Chou, C.-T. CO₂ capture from flue gas of a coal-fired power plant using three-bed PSA process. *Energies* **2021**, *14*, 3582. [[CrossRef](#)]
45. Xie, W. Uncertainty analysis and evaluation of calibration results of meteorological chromatograph. In Proceedings of the 2022 IEEE 10th Joint International Information Technology and Artificial Intelligence Conference (ITAIC), Chongqing, China, 17–19 June 2022; pp. 1158–1161.
46. Quan, C.; Xu, S.; An, Y.; Liu, X. Co-pyrolysis of biomass and coal blend by TG and in a free fall reactor. *J. Therm. Anal. Calorim.* **2014**, *117*, 817–823. [[CrossRef](#)]
47. Leng, L.; Xiong, Q.; Yang, L.; Li, H.; Zhou, Y.; Zhang, W.; Jiang, S.; Li, H.; Huang, H. An overview on engineering the surface area and porosity of biochar. *Sci. Total Environ.* **2021**, *763*, 144204. [[CrossRef](#)]
48. Pikkor, H.; Maaten, B.; Baird, Z.S.; Järvi, O.; Konist, A.; Lees, H. Surface area of oil shale and its solid pyrolysis products depending on the particle size. *Chem. Eng. Trans.* **2020**, *81*, 961–966.

Disclaimer/Publisher’s Note: The statements, opinions and data contained in all publications are solely those of the individual author(s) and contributor(s) and not of MDPI and/or the editor(s). MDPI and/or the editor(s) disclaim responsibility for any injury to people or property resulting from any ideas, methods, instructions or products referred to in the content.